PROCEEDINGS OF SPIE

SPIEDigitalLibrary.org/conference-proceedings-of-spie

Transient photoconductivity and photo-excited carrier dynamics in (Bi1-xlnx)2Se3 thin films

Shi, Teng, Kushnir, Kateryna, Wang, Zhengtianye, Law, Stephanie, Titova, Lyubov

Teng Shi, Kateryna Kushnir, Zhengtianye Wang, Stephanie Law, Lyubov Titova, "Transient photoconductivity and photo-excited carrier dynamics in (Bi1-xlnx)2Se3 thin films," Proc. SPIE 11278, Ultrafast Phenomena and Nanophotonics XXIV, 112780H (27 February 2020); doi: 10.1117/12.2546692



Event: SPIE OPTO, 2020, San Francisco, California, United States

Transient photoconductivity and photoexcited carrier dynamics in (Bi_{1-x}In_x)₂Se₃ thin films

Teng Shia*, Kateryna Kushnira, Zhengtianye Wangb, Stephanie Lawb, Lyubov Titova

^aDepartment of Physics, Worcester Polytechnic Institute, Worcester, MA, 01609, USA; ^bDepartment of Materials Science and Engineering, University of Delaware, 127 The Green Room 201, Newark, DE 19716, USA

*E-mail: tshi@wpi.edu

ABSTRACT

We use time-resolved THz spectroscopy to study microscopic conductivity and photoinduced carrier dynamics in MBE-grown 100 nm thick $(Bi_{1-x}In_x)_2Se_3$ thin films with indium concentration varying from x=0 to x=0.5. Both intrinsic and photoinduced conductivity in Bi2Se3 is significantly higher compared to the films with x=0.25 and x=0.50, with carriers that are not constrained by the twin domain boundaries and exhibit high mobility of 1100 cm²/Vs. We find that introducing indium with concentration of x=0.25 and higher, above the threshold for a topological to trivial transition, suppresses both intrinsic and photoinduced conductivity by over an order of magnitude and reduces the lifetime of photoexcited carriers. These findings demonstrate that controlling indium concentration in $(Bi_{1-x}In_x)_2Se_3$ films provides an avenue to design $(Bi_{1-x}In_x)_2Se_3$ films with desired properties for high-speed optoelectronic devices.

Keywords: topological insulator, thin film, terahertz spectroscopy, photoconductivity, ultrafast carrier dynamics

1. INTRODUCTION

Topological insulators (TI), a newly discovered state of matter, have attracted wide attention due to their unique band structures that combine a bulk band gap with gapless surface states with linear dispersion [1-3]. Two-dimensional surface Dirac electrons exhibit spin-momentum locking, resulting in a significant reduction in backscattering [4]. These features of TIs offer opportunities for the development of spintronic, thermoelectric and optoelectronic applications [5-10]. Bi₂Se₃ is a particularly attractive TI, due to its simple topological surface states and small bulk bandgap \sim 0.3 eV [1,11,12]. An ability to combine a TI material in a heterostructure with a lattice-matched trivial band insulator (BI) greatly expands the application possibilities, and in the case of Bi₂Se₃, (Bi_{1-x}In_x)₂Se₃ alloy is an ideal BI counterpart as it undergoes a phase transition from TI to BI for x>0.06 [13-17]. In a recent study, we have successfully grown (Bi_{1-x}In_x)₂Se₃ films with various indium concentrations by molecular beam epitaxy, and investigated the effect of In concentration on the optical properties. We found linear relationships between the In concentration, lattice constant, and both direct and indirect optical band gaps across the composition range of $0 \le x \le 1$ [12].

Here, we focus on the effect of In concentration on ultrafast photoexcited carrier dynamics and microscopic conductivity, which is critical for applications of TIs and lattice-compatible BIs in high-speed optoelectronic devices. Recently, ultrafast carrier relaxation in Bi₂Se₃ thin films and crystals has been investigated, with sub-picosecond time resolution, using transient reflectivity measurements [18-20]. These studies found that defect-induced charge carrier trapping and electron – phonon interactions play important roles in the ultrafast carrier dynamics in TI Bi₂Se₃. In addition, several optical pump-THz probe spectroscopy have demonstrated that it is possible to distinguish contributions of the bulk and surface states to the overall photoconductivity of thin Bi₂Se₃ films, and revealed, among other findings, that at high temperatures (>230 K),

Ultrafast Phenomena and Nanophotonics XXIV, edited by Markus Betz, Abdulhakem Y. Elezzabi, Proc. of SPIE Vol. 11278, 112780H ⋅ © 2020 SPIE CCC code: 0277-786X/20/\$21 ⋅ doi: 10.1117/12.2546692

photoexcited carriers scatter to the highly conductive surface states [21-23]. Furthermore, THz time-domain spectroscopy has recently applied to probe the changes in carrier scattering time in $(Bi_{1-x}In_x)_2Se_3$ as a function of In concentration across the TI-BI phase transition.

In this paper, we report on optical pump - THz probe measurements on $(Bi_{1-x}In_x)_2Se_3$ thin films with indium concentration ranging from x=0 to x=0.5, and we find that indium content above the TI-BI transition substantially decreases not only the intrinsic conductivity but also the photoconductivity.

2. MATERIAL GROWTH

(Bi_{1-x}In_x)₂Se₃ thin films were synthesized on c-plane sapphire with a selenium cracking source in a dedicated Veeco GenXplor molecular beam epitaxy (MBE) chamber. During the growth process, the selenium flux is fixed constant, while the bismuth and indium fluxes and the substrate temperature are adjusted in order to achieve different compositions. Reflection high energy electron diffraction (RHEED) is used to monitor the crystal quality during growth. Similar RHEED patterns indicate that all thin films are single phase with high crystal quality. More detailed information about thin film growth can be found elsewhere [13,14].

We show a set of AFM images of 100 nm thick $(Bi_{1-x}In_x)_2Se_3$ thin films with indium concentration of 0, 0.25 and 0.5 respectively, in Figure 1. Images of all samples show evidence of domains, with smaller domains in Bi_2Se_3 (Fig.1(a)), and larger domains that are flatter in $(Bi_{1-x}In_x)_2Se_3$ with x=0.25 and x=0.5 (Fig. 1(b) and (c)). Previous measurements showed that both the lattice constant and optical bandgap vary linearly as a function of indium concentration [12].

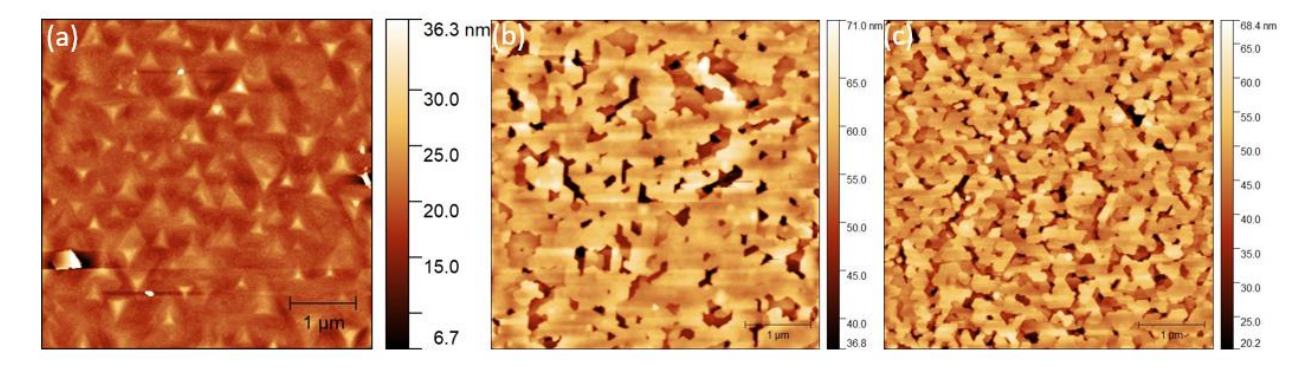


Figure 1. AFM images of $(Bi_{1-x}In_x)_2Se_3$ thin films with indium concentration of (a) x=0, (b) x=0.25 and (c) x=0.50 show domains in all three samples.

3. EXPERIMENTAL METHODS

THz spectroscopy

Here we utilize THz time-domain spectroscopy and time-resolved THz spectroscopy to study the equilibrium and non-equilibrium free carrier dynamics of $(Bi_{1-x}In_x)_2Se_3$ thin films. THz probe pulses was generated by optical rectification of 800 nm, 100 fs pulses from a 1 kHz amplified Ti:sapphire laser in a 1mm thick [110] ZnTe crystal. The THz probe beam of 1.5 mm diameter was focused onto the sample at normal incidence by a set of off-axis parabolic mirrors. THz pulses transmitted through the sample were detected in a second ZnTe crystal by electro-optic sampling. For optical pump – THz probe measurements, samples were photoexcited by 400 nm (3.1 eV) pulses, ensuring excitation above the direct band gap in all studied films.

4. EXPERIMENTAL RESULTS AND DISCUSSION

In Figure 2, the left column shows the intrinsic frequency-resolved complex conductivity spectra of Bi_2Se_3 (Fig. 2(a)), $(Bi_{0.75}In_{0.25})_2Se_3$ (Fig 2(c)) and $(Bi_{0.50}In_{0.50})_2Se_3$ (Fig 2(e)), obtained using THz TDS. A clear signature of an α -phonon mode can be observed in Bi_2Se_3 and $(Bi_{0.75}In_{0.25})_2Se_3$ films, in agreement with other studies that demonstrated an α -phonon in 2.17-2.90 THz range (or, equivalently, 9-12 meV) in $(Bi_{1-x}In_x)_2Se_3$ with indium content ≤ 0.5 and a linear relationship between the phonon frequency and the indium concentration.[17,21-22]. The phonon signature in Bi_2Se_3 is super-imposed with the Drude-like free carrier conductivity that is orders of magnitude higher than in $(Bi_{0.75}In_{0.25})_2Se_3$ and $(Bi_{0.50}In_{0.50})_2Se_3$ films, leading us to attribute the high free carrier conductivity in Bi_2Se_3 to the topological surface carriers. Despite similar morphology and high crystallinity, we observe nearly zero DC conductivity in $(Bi_{0.75}In_{0.25})_2Se_3$ and $(Bi_{0.50}In_{0.50})_2Se_3$ films, which are expected to be conventional BIs.

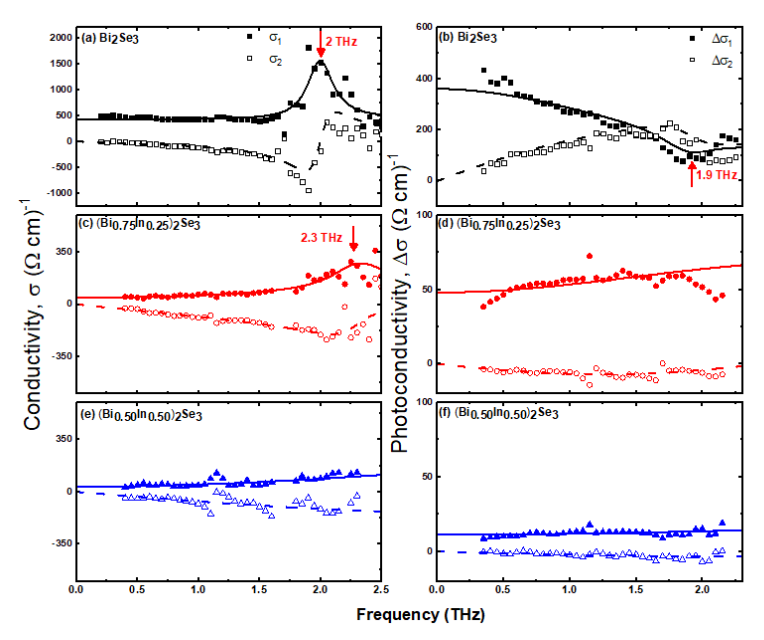


Figure 2. Left column: Complex THz conductivity of Bi₂Se₃ (a), (Bi_{0.75}In_{0.25})₂Se₃ (c) and (Bi_{0.50}In_{0.50})₂Se₃ (e) films. Symbols represent the experimental data and lines are the global fit of real (solid lines) and imaginary (dash lines) conductivity to Drude-Smith-Lorentz model; Right column: change in complex THz conductivity at 5 ps after excitation for Bi₂Se₃ (b), (Bi_{0.75}In_{0.25})₂Se₃ (d) and (Bi_{0.50}In_{0.50})₂Se₃ (f) films.

The right column of Figure 2 shows the transient photoconductivity in all three films as a time delay of 5 ps following excitation with 400 nm, ~ 100 fs pulses with a fluence of $160 \,\mu\text{J/cm}^2$ in Bi₂Se₃ (Figure 2 (b), (Bi_{0.75}In_{0.25})₂Se₃ (Figure 2(d)), and (Bi_{0.50}In_{0.50})₂Se₃ (Figure 2(f)). Again, like in the case of intrinsic conductivity, transient photoconductivity is over an order of magnitude higher in Bi₂Se₃ compared to (Bi_{0.75}In_{0.25})₂Se₃ and (Bi_{0.50}In_{0.50})₂Se₃. To describe the free carrier THz conductivity, we apply a phenomenological Drude-Smith model which has been successfully applied to various material systems with domains, disorder and grain boundaries that results in localization of free carriers over distances commensurate with their mean free path [24-26]. In this model, complex conductivity is expressed as

$$\tilde{\sigma}_{DS}(\omega) = \frac{Ne^2 \tau_{DS}}{m^* (1 - i\omega \tau_{DS})} \left(1 + \frac{c}{1 - i\omega \tau_{DS}}\right),$$

where N, e and m^* represent the charge carrier density, electronic charge and the effective mass of the charge carriers, respectively. Carrier scattering time in Drude-Smith model is represented as τ_{DS} , and c is the localization parameter which can vary in the range of -1 to 0. Localization parameter is a measure of carrier localization over the probed scale lengths. Cocker et al. have provided a thorough discussion of microscopic origin of Drude-Smith model in Ref [27]. In order to account for phonon-related effects observed in Bi₂Se₃ and (Bi_{0.75}In_{0.25})₂Se₃ films, we introduce a Lorentzian contribution to the Drude-Smith conductivity. The resulting global fits of real and imaginary components of conductivity are shown in Figure 2 as solid and dashed lines, respectively.

We find that free carrier response in photoconductivity of Bi_2Se_3 is well described by the Drude-Smith formula with c=0, which represents Drude-like conductivity of carrier that are not susceptible to scattering by the domain or grain boundaries. This observation is again consistent with topologically protected surface states being a dominant contribution to THz conductivity of Bi_2Se_3 even at room temperature. We also find that optical excitation results in a redshift of the α -phonon mode, evidenced by a negative Lorentzian contribution at 1.9 THz. This redshift may be attributed to a combination of transient temperature increase due to the laser excitation and a shift due to enhanced carrier-phonon coupling [22,23]. Photoexcited carrier scattering time in Bi_2Se_3 5 ps after excitation with $\sim 160~\mu\text{J/cm}^2$ pulses is $\sim 90~\text{fs}$, corresponding to a high average carrier mobility of $1100~\text{cm}^2/\text{Vs}$, calculated using an effective mass of $0.15m_0$ [28-30]. On the other hand, photoconductivity of In-containing films shows pronounced effect of localization by the domain boundaries with c parameter of $\sim -0.65~\text{for}~(Bi_{0.75}In_{0.25})_2Se_3$ and $-0.75~\text{for}~(Bi_{0.50}In_{0.50})_2Se_3$. Carrier scattering time, and correspondingly, the short-range, intra-domain mobility of photoexcited carriers is also significantly reduced in these films, with τ_{DS} of $\sim 35~\text{fs}$ for $(Bi_{0.75}In_{0.25})_2Se_3$ and $\sim 20~\text{fs}$ for $(Bi_{0.50}In_{0.50})_2Se_3$. The reduction if carrier scattering time with increase in In concentration suggests that increased disorder introduced by In reduces carrier mobility.

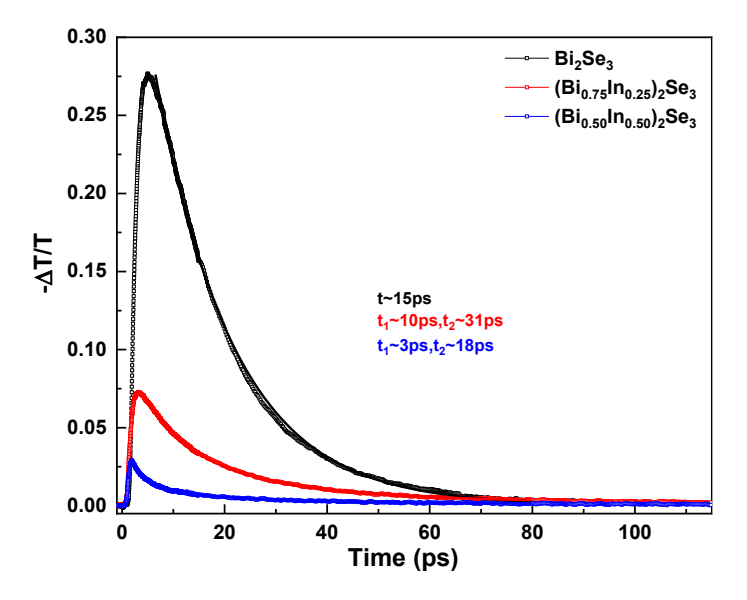


Figure 3. Change in transmission of the main peak of THz probe pulse in $(Bi_{1-x}In_x)_2Se_3$ thin films as a function of delay time with a fluence of $160 \mu J/cm^2$ photoexcited by 400 nm.

In Figure 3, we show the transient change in transmission of the main peak of THz probe pulse $(-\Delta T/T)$ in $(Bi_{1-x}In_x)_2Se_3$ thin films as a function of delay time between the optical pump and THz probe pulse (shown as symbols) at the same pump fluence, which is proportional to the time-dependent photoconductivity [24]. Transient supression of THz peak transmission photoexcited at $160 \ \mu J/cm^2$ as a function of indium concentration has been observed as expected. Solid lines are the fits of the experimental data using the exponential function given by $\frac{\Delta T(t)}{T} = A_0 + A_1 \exp\left(-\frac{t}{t_1}\right) + A_2 \exp\left(-\frac{t}{t_2}\right)$. t_1 and t_2 are the decay times, while A_1 and A_2 are the corresponding amplitudes. For Bi_2Se_3 , we observe a single

exponential decay with $t_1 = 15$ ps as photoexcited carriers are trapped and/or recombine. For indium-containing films, the observed photoconductivity decays are bi-exponential. $(Bi_{0.75}In_{0.25})_2Se_3$ exhibits a fast component of 10 ps, followed by a small contribution of a slower decay with ~31 ps decay time. For $(Bi_{0.50}In_{0.50})_2Se_3$, the fast decay component decreases to only ~3 ps, and a slower component of 18 ps. In both indium-containing films, overall photoconductivity is significantly lower than that in Bi_2Se_3 at the same excitation conditions, suggesting that most photoexcited carriers are trapped or recombine within a short period of time (~ sub-picoseconds) after photoexcitation, consistent with previous study on ultrafast carrier relaxation in Bi_2Se_3 [18-20].

5. SUMMARY

Our work demonstrates how indium content impacts conductivity and carrier dynamics in $(Bi_{1-x}In_x)_2Se_3$ films. It shows a 30-fold suppression in intrinsic conductivity of $(Bi_{0.50}In_{0.50})_2Se_3$ compared to Bi_2Se_3 . Our results suggest that both intrinsic and photoinduced conductivity in Bi_2Se_3 is dominated by the carriers in topological surface states that are not susceptible to domain-boundary scattering. On the other hand, domain boundaries lead to significant carrier confinement in both indium-containing BI films. These findings demonstrate that controlling indium concentration in $(Bi_{1-x}In_x)_2Se_3$ films provides an avenue to design $(Bi_{1-x}In_x)_2Se_3$ films and TI/BI heterostructures with desired properties for high-speed optoelectronic devices.

REFERENCES

- [1] Xia, Y., Qian, D., Hsieh, D., Wray, L., Pal, A., Lin, H., Bansil, A., Grauer, D., Hor, Y. S., Cava, R. J. and Hasan, M. Z., "Observation of a large-gap topological-insulator class with a single Dirac cone on the surface," Nat. Phys. **5**(6),398–402 (2009).
- [2] Hsieh, D., Xia, Y., Qian, D., Wray, L., Dil, J. H., Meier, F., Osterwalder, J., Patthey, L., Checkelsky, J. G., Ong, N. P., Fedorov, A. V., Lin, H., Bansil, A., Grauer, D., Hor, Y. S., Cava, R. J. and Hasan, M. Z., "A tunable topological insulator in the spin helical Dirac transport regime," Nature **460**(7259), 1101–1105 (2009).
- [3] Hasan, M. Z., & Kane, C. L. Colloquium: topological insulators. Reviews of modern physics, 82(4), 3045(2010).
- [4] Kim, D., Cho, S., Butch, N. P., Syers, P., Kirshenbaum, K., Adam, S., Paglione, J. and Fuhrer, M. S., "Surface conduction of topological Dirac electrons in bulk insulating Bi₂Se₃," Nat. Phys. **8**(6), 459–463 (2012).
- [5] Pesin, D. and MacDonald, A. H., "Spintronics and pseudospintronics in graphene and topological insulators," Nat. Mater. 11(5), 409–416 (2012).
- [6] Hor, Y. S., Richardella, A., Roushan, P., Xia, Y., Checkelsky, J. G., Yazdani, A., Hasan, M. Z., Ong, N. P. and Cava, R. J., "P-type Bi₂Se₃ for topological insulator and low-temperature thermoelectric applications," Phys. Rev. B Condens. Matter Mater. Phys. **79**(19), 2–6 (2009).
- [7] Zhang, X., Wang, J. and Zhang, S. C., "Topological insulators for high-performance terahertz to infrared applications," Phys. Rev. B Condens. Matter Mater. Phys. **82**(24), 1–5 (2010).
- [8] Peng, H., Dang, W., Cao, J., Chen, Y., Wu, D., Zheng, W., and Liu, Z. "Topological insulator nanostructures for near-infrared transparent flexible electrodes." *Nature chemistry*, 4(4), 281(2012).
- [9] Liu, H., Zheng, X.-W., Liu, M., Zhao, N., Luo, A.-P., Luo, Z.-C., Xu, W.-C., Zhang, H., Zhao, C.-J. and Wen, S.-C., "Femtosecond pulse generation from a topological insulator mode-locked fiber laser," Opt. Express 22(6), 6868 (2014).
- [10] Zhang, H., Zhang, X., Liu, C., Lee, S. T., and Jie, J. "High-responsivity, high-detectivity, ultrafast topological insulator Bi₂Se₃/silicon heterostructure broadband photodetectors." *ACS nano*, 10(5), 5113-51 (2016).
- [11] Nechaev, I. A., Hatch, R. C., Bianchi, M., Guan, D., Friedrich, C., Aguilera, I., Mi, J. L., Iversen, B. B., Blügel, S., Hofmann, P. and Chulkov, E. V., "Evidence for a direct band gap in the topological insulator Bi₂Se₃ from theory and experiment," Phys. Rev. B Condens. Matter Mater. Phys. **87**(12), 1–5 (2013).
- [12] Wang, Y. and Law, S., "Optical properties of (Bi_{1-x}In_x)₂Se₃ thin films," Opt. Mater. Express 8(9), 2570 (2018).
- [13] Ginley, T. P. and Law, S., "Growth of Bi₂Se₃ topological insulator films using a selenium cracker source," J. Vac. Sci. Technol. B, Nanotechnol. Microelectron. Mater. Process. Meas. Phenom. **34**(2), 02L105 (2016).
- [14] Wang, Y., Ginley, T. P. and Law, S., "Growth of high-quality Bi₂Se₃ topological insulators using (Bi_{1-x}In_x)₂Se₃ buffer layers," J. Vac. Sci. Technol. B, Nanotechnol. Microelectron. Mater. Process. Meas. Phenom. **36**(2), 02D101 (2018).
- [15] Zhao, Y., Liu, H., Guo, X., Jiang, Y., Sun, Y., Wang, H., Wang, Y., Li, H. D., Xie, M. H., Xie, X. C. and Wang, J., "Crossover from 3D to 2D quantum transport in Bi₂Se₃/In₂Se₃ superlattices," Nano Lett. **14**(9), 5244–5249 (2014).
- [16] Wang, Z. Y., Guo, X., Li, H. D., Wong, T. L., Wang, N. and Xie, M. H., "Superlattices of Bi₂Se₃/In₂Se₃: Growth characteristics and structural properties," Appl. Phys. Lett. **99**(2), 2011–2014 (2011).
- [17] Wu, L., Brahlek, M., Aguilar, R. V., Stier, A. V., Morris, C. M., Lubashevsky, Y., Bilbro, L. S., Bansal, N., Oh, S. and Armitage, N. P., "A sudden collapse in the transport lifetime across the topological phase transition in (Bi_{1-x}In_x)₂Se₃," Nat. Phys. **9**(7), 410–414 (2013).
- [18] Glinka, Y. D., Babakiray, S., Johnson, T. A., Holcomb, M. B. and Lederman, D., "Effect of carrier recombination on ultrafast carrier dynamics in thin films of the topological insulator Bi₂Se₃," Appl. Phys. Lett. **105**(17), 0–5 (2014).
- [19] Glinka, Y. D., Babakiray, S., Johnson, T. A., Bristow, A. D., Holcomb, M. B. and Lederman, D., "Ultrafast carrier dynamics in thin-films of the topological insulator Bi2Se3," Appl. Phys. Lett. **103**(15), 0–5 (2013).
- [20] Qi, J., Chen, X., Yu, W., Cadden-Zimansky, P., Smirnov, D., Tolk, N. H., Miotkowski, I., Cao, H., Chen, Y. P., Wu, Y., Qiao, S. and Jiang, Z., "Ultrafast carrier and phonon dynamics in Bi₂Se₃ crystals," Appl. Phys. Lett. **97**(18), 1–4 (2010). [21] Park, B. C., Kim, T. H., Sim, K. I., Kang, B., Kim, J. W., Cho, B., Jeong, K. H., Cho, M. H. and Kim, J. H., "Terahertz single conductance quantum and topological phase transitions in topological insulator Bi₂Se₃ ultrathin films," Nat. Commun. **6**(May 2014), 1–8 (2015).
- [22] Valdés Aguilar, R., Qi, J., Brahlek, M., Bansal, N., Azad, A., Bowlan, J., Oh, S., Taylor, A. J., Prasankumar, R. P. and Yarotski, D. A., "Time-resolved terahertz dynamics in thin films of the topological insulator Bi₂Se₃," Appl. Phys. Lett. **106**(1), 19–24 (2015).
- [23] Sim, S., Brahlek, M., Koirala, N., Cha, S., Oh, S. and Choi, H., "Ultrafast terahertz dynamics of hot Dirac-electron surface scattering in the topological insulator Bi2 Se3," Phys. Rev. B Condens. Matter Mater. Phys. **89**(16), 1–8 (2014).

- [24] Titova, L. V., Cocker, T. L., Cooke, D. G., Wang, X., Meldrum, A. and Hegmann, F. A., "Ultrafast percolative transport dynamics in silicon nanocrystal films," Phys. Rev. B Condens. Matter Mater. Phys. **83**(8), 1–9 (2011). [25] Cocker, T. L., Titova, L. V., Fourmaux, S., Holloway, G., Bandulet, H. C., Brassard, D., Kieffer, J. C., El Khakani, M. A. and Hegmann, F. A., "Phase diagram of the ultrafast photoinduced insulator-metal transition in vanadium dioxide," Phys. Rev. B Condens. Matter Mater. Phys. **85**(15), 1–11 (2012).
- [26] Titova, L. V., Cocker, T. L., Xu, S., Baribeau, J. M., Wu, X., Lockwood, D. J. and Hegmann, F. A., "Ultrafast carrier dynamics and the role of grain boundaries in polycrystalline silicon thin films grown by molecular beam epitaxy," Semicond. Sci. Technol. **31**(10) (2016).
- [27] Cocker, T. L., Baillie, D., Buruma, M., Titova, L. V., Sydora, R. D., Marsiglio, F. and Hegmann, F. A., "Microscopic origin of the Drude-Smith model," Phys. Rev. B **96**(20) (2017).
- [28] Analytis, J. G., Chu, J. H., Chen, Y., Corredor, F., McDonald, R. D., Shen, Z. X. and Fisher, I. R., "Bulk Fermi surface coexistence with Dirac surface state in Bi₂Se₃: A comparison of photoemission and Shubnikov-de Haas measurements," Phys. Rev. B Condens. Matter Mater. Phys. **81**(20), 1–5 (2010).
- [29] Orlita, M., Piot, B. A., Martinez, G., Kumar, N. K. S., Faugeras, C., Potemski, M., Michel, C., Hankiewicz, E. M., Brauner, T., Drašar, Schreyeck, S., Grauer, S., Brunner, K., Gould, C., Brüne, C. and Molenkamp, L. W., "Magneto-Optics of Massive Dirac Fermions in Bulk Bi₂Se₃," Phys. Rev. Lett. **114**(18), 1–6 (2015).
- [30] Zhu, J., Liu, F., Zhou, S., Franke, C., Wimmer, S., Volobuev, V. V., Springholz, G., Pashkin, A., Schneider, H. and Helm, M., "Lattice vibrations and electrical transport in (Bi_{1-x}In_x)₂Se₃ films," Appl. Phys. Lett. **109**(20) (2016).